Brain Stimulation 9 (2016) 594–600

Contents lists available at ScienceDirect

Brain Stimulation

journal homepage: www.brainstimjrnl.com

Investigating the Causal Role of rOFA in Holistic Detection of Mooney Faces and Objects: An fMRI-guided TMS Study

Silvia Bona [a,b,c,d], Zaira Cattaneo [e,f,*], Juha Silvanto [g,*]

[a] Department of Neuroscience and Biomedical Engineering, Aalto University School of Science, 00076 Espoo, Finland
[b] Advanced Magnetic Imaging Centre, Aalto Neuroimaging, OV Lounasmaa Laboratory, School of Science, Aalto University, 00076 Espoo, Finland
[c] BioMag Laboratory, HUS Medical Imaging Center, Helsinki University Central Hospital, 00290 Helsinki, Finland
[d] Department of Behavioural Sciences, University of Helsinki, 00014 Helsinki, Finland
[e] Department of Psychology, University of Milano-Bicocca, 20126 Milan, Italy
[f] Brain Connectivity Center, National Neurological Institute C. Mondino, 27100 Pavia, Italy
[g] Department of Psychology, Faculty of Science and Technology, University of Westminster, 309 Regent Street, W1B 2HW London, UK

ARTICLE INFO

Article history:
Received 25 November 2015
Received in revised form 15 January 2016
Accepted 6 April 2016
Available online 8 April 2016

Keywords:
Face processing
Object processing
Holistic detection
fMRI-guided TMS
Visual cortex
Occipital face area

ABSTRACT

Background: The right occipital face area (rOFA) is known to be involved in face discrimination based on *local featural* information. Whether this region is also involved in *global, holistic* stimulus processing is not known.
Objective: We used fMRI-guided transcranial magnetic stimulation (TMS) to investigate whether rOFA is causally implicated in stimulus detection based on holistic processing, by the use of Mooney stimuli.
Methods: Two studies were carried out: In Experiment 1, participants performed a detection task involving Mooney faces and Mooney objects; Mooney stimuli lack distinguishable local features and can be detected solely via holistic processing (i.e. at a global level) with top-down guidance from previously stored representations. Experiment 2 required participants to detect shapes which are recognized via bottom-up integration of local (collinear) Gabor elements and was performed to control for specificity of rOFA's implication in holistic detection.
Results: In Experiment 1, TMS over rOFA and rLO impaired detection of all stimulus categories, with no category-specific effect. In Experiment 2, shape detection was impaired when TMS was applied over rLO but not over rOFA.
Conclusions: Our results demonstrate that rOFA is causally implicated in the type of top-down holistic detection required by Mooney stimuli and that such role is not face-selective. In contrast, rOFA does not appear to play a causal role in detection of shapes based on bottom-up integration of local components, demonstrating that its involvement in processing non-face stimuli is specific for holistic processing.

Introduction

The occipital face area (OFA), located in the lateral inferior occipital gyrus, is a key component of the face-processing network (e.g. References 1–5) typically showing a more robust face-response in the right hemisphere [6–8]. In particular, OFA is involved in the encoding of face parts (or so-called facial featural information) such as eyes, nose and mouth (e.g. References 9–11). Accordingly, stimulating right OFA (rOFA) with transcranial magnetic stimulation (TMS) has been found to impair participants' ability in discriminating faces (but not objects) differing by single components (such as the shape of the eyes and the mouth), without affecting the processing of configural information such as the spacing between face parts [12]. These findings suggest that rOFA is important for building up an initial structural representation based on local properties, prior to subsequent processing of more complex aspects occurring in higher-level face areas such as the fusiform face area (FFA) [2,8]. Nonetheless, FFA can be activated even in the absence of input from rOFA, suggesting that OFA may rather respond to re-entrant feedback from higher-level face areas where an initial coarse representation would be constructed [4,13–15]. In line with this, following TMS over rOFA, participants were impaired in face identity discrimination but not in distinguishing intact from scrambled faces [16].

Notwithstanding the important role played by rOFA at different stages of face processing, there is also evidence suggesting that rOFA may be important in processing of non-face stimuli (e.g. References 17–20). Furthermore, prior TMS evidence has shown that

* Corresponding authors. Tel.: +44 (0)20 7911 5000 (J. Silvanto).
E-mail addresses: zaira.cattaneo@unimib.it (Z. Cattaneo), j.silvanto@westminster.ac.uk (J. Silvanto).

http://dx.doi.org/10.1016/j.brs.2016.04.003

rOFA plays a causal role in symmetry discrimination, both in faces and in dot patterns [21], raising the possibility that this region is important for extracting global "Gestalt" stimulus properties. Such attributes play an important role in holistic processing, which refers to stimulus detection in which recognition of the "whole" precedes detection of the single elements (e.g. Reference 22). Holistic processing is believed to be based on top-down guidance by previously stored representations (as opposed to bottom-up extraction of local features) (e.g. Reference 23). Such holistic processing is required for the detection of Mooney stimuli [24] which are two-tone (black-and-white) images lacking in distinguishable local facial features and which can be recognized solely on the basis of their global Gestalt [22,25–27].

Whether rOFA is involved in such holistic detection is not known. In the present study, we used online fMRI-guided transcranial magnetic stimulation (cf. Reference 28; for a review, see References 29–31) to investigate this issue. In Experiment 1 we tested three Mooney stimulus categories: faces, guitars and objects. TMS was applied either over the rOFA, the rLO or vertex (control site) while participants performed the Mooney detection task. In a second experiment we used the same TMS parameters but during a shape detection task based on integration of local elements (collinear Gabor patches): this experiment was a direct replication of the experiment reported in Reference 21 and aimed to control for specificity of rOFA involvement in *holistic* processing.

Experiment 1

Materials and methods

Participants

Fifteen students (8 males, mean age = 24.3, SD = 2.07) from Aalto University, Espoo (Finland) took part in Experiment 1. All participants were right-handed [32] and had normal or corrected-to-normal vision. The study was approved by the local ethics committee and participants were treated in accordance with the Declaration of Helsinki. Participants provided a written informed consent and were screened for contraindications to fMRI and TMS. Each participant underwent three sessions: in the first session, the fMRI localization was carried out. The TMS experiments were performed in the remaining two sessions: specifically, Experiment 1 was performed in the second session and Experiment 2 in the third session.

fMRI localization of LO and OFA

A 3T MAGNETOM Skyra whole-body scanner (Siemens Healthcare, Erlangen, Germany) equipped with a 30-channel head–neck coil was used to acquire the functional volumes. The session consisted of 3 runs (one run for LO and two runs for OFA). Stimuli for the LO localizer were gray-scale images of common objects and scrambled objects; for OFA localizers, faces and objects were used. Scrambled objects were obtained by randomly selecting an equal number of square tiles from the original object images and arranging them in a 16×16 grid of the same dimensions as the object images. All stimuli were presented in the middle of the screen on an 18-inch monitor with a display resolution of 1280×1024. Viewing distance was 40 cm. rLO was defined as the activation peak of cluster of voxels that responded more to objects versus scrambled objects (see References 21,33 for similar procedure). Functional images were acquired in a single run lasting 432 sec with gradient echo sequence (23 slices with 3.5 mm slice thickness, RT = 2 s, echo time = 30 ms, voxel size = $3.125 \times 3.125 \times 3$ mm^3, flip angle = 75). rOFA was defined as the activation peak of the cluster of voxels that responded more to faces versus objects. Functional images were collected over 2 runs, each lasting 271.2 sec. Otherwise, the same parameters as for rLO localization were used. For each participant, a high resolution T1 weighted MPRAGE anatomical scan was also collected. Data preprocessing, parameter estimation and visualization were performed with SPM8 MatlabTM toolbox (http://www.fil.ion.ucl.ac.uk/spm, cf. Reference 34). The first four slices of each run were removed to ensure a stable magnetization and subsequent functional images were corrected for slice acquisition order and head movements. During the parameter estimation, the data were high-pass filtered with 128 s cutoff, and noise autocorrelation was modeled with AR(1) model. The data were coregistered with the high-resolution anatomical images. The mean MNI coordinates were: *rOFA*: 39 (SD 4.7), –81 (SD 9.7), –10 (SD 2.8); *rLO*: 46 (SD 3.5), –75 (SD 4.1), –4 (SD 6.7); these coordinates are consistent with those found in prior fMRI-guided TMS studies on rOFA and rLO function (e.g. References 35,36). Fig. 1 shows the rOFA and rLO sites in a representative participant.

TMS stimulation

TMS pulses were delivered through a biphasic figure-of-eight coil connected to a Nexstim stimulator (Nexstim Ltd., Helsinki, Finland). The eXimia NBS neuronavigation system (Nexstim Ltd., Helsinki, Finland), a co-registration software that allows real-time fMRI-guided positioning of the coil (e.g. References 37,38), was used to localize the stimulation sites. In each trial, participants received 3 pulses of TMS at a frequency of 10 Hz and an intensity of 40% of the maximum stimulator output over the stimulation sites, concurrently with visual target onset. These parameters were chosen on the basis of our previous study where we stimulated the same brain regions [21]. This stimulation intensity corresponds to approximately 80% of the phosphene threshold of the early visual cortex, which is in the region of 45–50% with the Nexstim stimulator and has been used in previous work in our laboratory [21,33,39]. A fixed TMS intensity has been used in most prior studies of OFA function (e.g. References 12,21,35). During the stimulation, the coil was held tangentially over the activation peaks obtained from participants' fMRI localizers, with the coil handle pointing upwards and parallel to the midline (e.g. References 36,40). Vertex was identified as the halfway point between the inion and the nasion and equidistant from the left and right intertragal notches [12,41] and was selected as control site to ensure that any TMS effect was not due to somatosensory sensations related to the stimulation (e.g. Cattaneo et al, 2012, 2015; Cattaneo & Silvanto, 2008).

Procedure

Participants performed a detection task with Mooney stimuli. The different Mooney categories (faces, guitars, objects) were tested in separated blocks.

Stimuli. We used 120 two-tone (black and white) Mooney images (40 Mooney faces, 40 Mooney guitars and 40 Mooney objects; see Fig. 2 for an example of each stimulus type). Each stimulus was approximately 15° in height and 10° in width. Mooney faces were drawn from the original set of "Mooney faces" created by Mooney [24]. Mooney guitars were selected from the original set of Castelhano et al. [42]; Mooney objects were selected from the original set of Imamoglu et al. [43] and consisted of pictures of animals, fruits and man-made objects. Mooney guitars are similar to faces in that they are a homogeneous stimulus class exhibiting clear prototypical shapes. Additionally, 40 meaningless images (i.e. non-face/guitar/object stimuli) were created for each of the three stimulus categories by dividing each item into a grid and randomly moving the positions of the squares.

Task. The time line of an experimental trial is shown in Fig. 2E. Stimuli were presented on an 18-inch monitor with a display

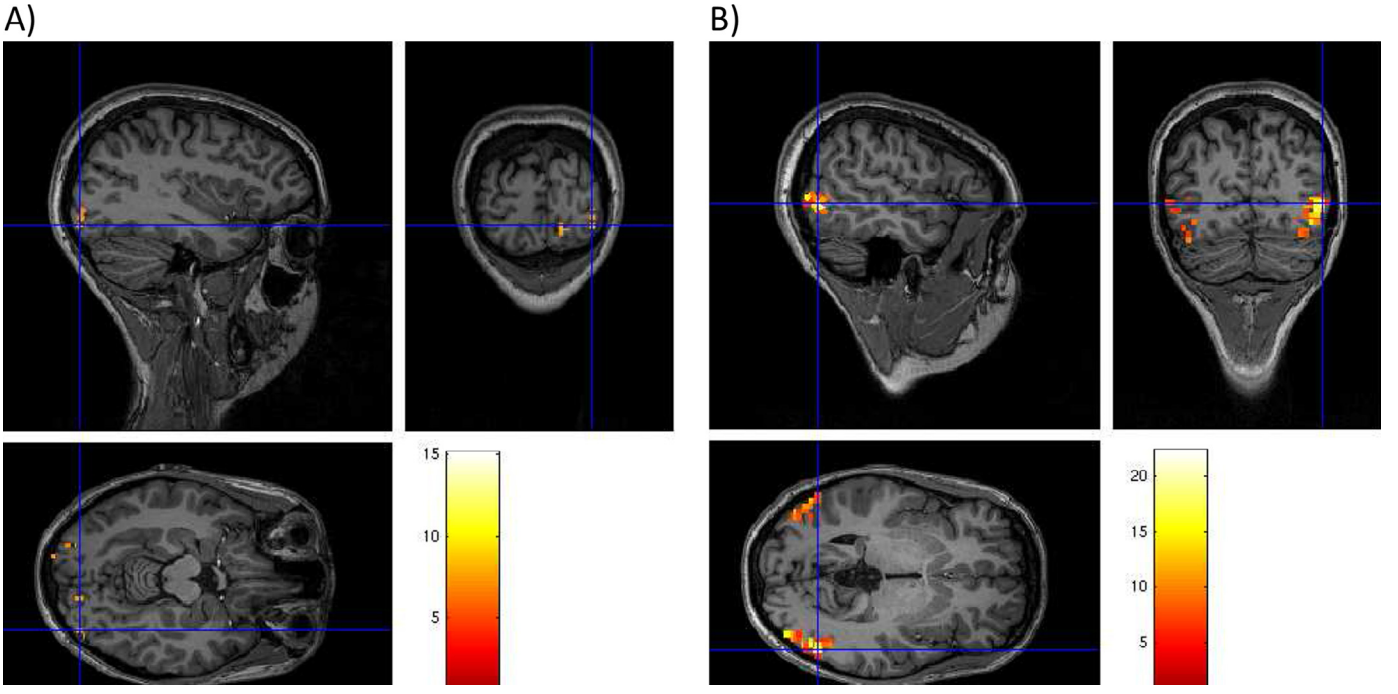

Figure 1. Axial, sagittal and coronal views (from bottom left in clockwise direction) of the activation peak for faces versus objects in rOFA (A) and objects versus scrambled objects in rLO (B).

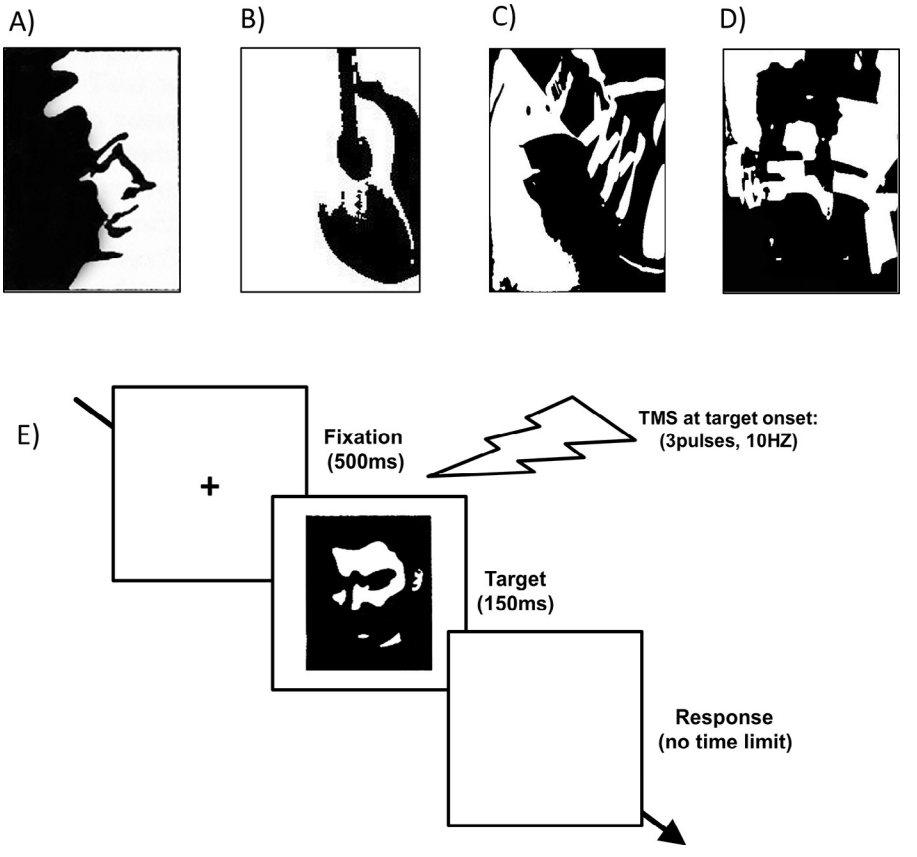

Figure 2. Experiment 1: Detection of Mooney stimuli. Example of A) a Mooney face; B) a Mooney guitar; C) a Mooney object (here a shoe); D) a scrambled Mooney stimulus (used for "target absent" trials); E) time line of an experimental trial. On each trial, participants were required to indicate whether or not a face/guitar/object was present. The different Mooney categories were tested in different blocks. On "target absent" trials, a scrambled Mooney stimulus was presented. The TMS pulse train (3 pulses, 10 Hz) began concurrently with the target onset.

resolution of 1600 × 1200 and participants were seated at a viewing distance of 60 cm, with their heads stabilized using a chin rest. Stimuli and task were controlled by E-Prime v2.0 (Psychology Software Tools Inc., Pittsburgh, USA). The different Mooney categories (faces, guitars and objects) were tested in different blocks, of which participants were informed in advance. Each trial started with a black fixation cross appearing in the middle of the screen for 500 ms, followed by either a target stimulus (i.e. a Mooney face, a Mooney guitar or a Mooney object, depending on the experimental block) or a scrambled Mooney stimulus. Faces and guitars were displayed for 150 ms, whereas objects appeared for 200 ms in order to reach a similar level of accuracy (80–90%) as with the other stimulus categories (stimulus durations were based on a prior behavioral pilot). Participants were asked to indicate, with a button press (using their right index and middle finger), whether the displayed stimulus was either a target stimulus (i.e. a face, guitar or object, depending on the experimental block) or a meaningless image. Both accuracy and response speed were emphasized. At target onset, a TMS pulse train (3 pulses at 10 Hz, i.e. pulse gap of 100 ms) was delivered over the rLO, the rOFA or vertex (baseline). For each stimulus category (faces, guitars and objects), participants performed three blocks, i.e. one block for each stimulation site (rLO, rOFA, and vertex). Therefore, nine blocks were carried out in total. Each block consisted of 80 trials (40 target stimuli and 40 meaningless pictures, presented in random order). The order of TMS blocks and the order of stimulus categories were randomized across participants, with the constraint that the three blocks of each stimulus category were always performed in a row, before moving to the next category. Prior to the experiment, participants carried out a brief practice session (with no TMS) for each stimulus category consisting of 20 trials (10 target stimuli and 10 meaningless pictures).

Results

Performance level was high in all conditions. Mean accuracies were: *Mooney faces:* 86% (SD = 1.01), *Mooney guitars:* 86% (SD = 1.74) and *Mooney objects*: 81% (SD = 2.47). Statistical analyses were carried out on reaction times (RT) of correct responses. Fig. 3 shows the mean reaction times of correct responses for each TMS condition in each stimulus category. A 3 × 3 repeated-measure ANOVA with TMS site (rLO, rOFA, vertex) and stimulus category (Mooney faces, Mooney guitars and Mooney objects) as within-subjects variables revealed a significant main effect of TMS ($F(2,34) = 11.48$, $p < .001$, $\eta_p^2 = .41$). The main effect of stimulus category was not significant ($F(2,34) = 3.09$, $p = .06$, $\eta_p^2 = .15$), nor was the interaction TMS site by stimulus category ($F(4,68) = 1.98$, $p = .12$, $\eta_p^2 = .11$). Post-hoc *t*-tests (Bonferroni–Holm correction applied) showed that, relative to vertex, both rOFA TMS ($t(14) = 4.03$, $p = .002$) and rLO TMS ($t(14) = 4.03$, $p = .003$) impaired performance. Performance with rOFA TMS was worse than with rLO TMS ($t(14) = 2.34$, $p = .03$).

Experiment 2

The key finding of Experiment 1 is that rOFA plays a causal role in stimulus detection based on holistic encoding and that such involvement is not tied to any specific stimulus category. In Experiment 2 we aimed to assess whether the involvement of rOFA in object detection is restricted to holistic processing (as in the case of Mooney stimuli) or whether it extends also to circumstances when detection is mediated by other mechanisms (such as processing collinearity of single elements composing the pattern). To this purpose, participants performed a shape detection task on stimuli which was defined by a closed contour of similarly oriented Gabor elements (see Fig. 4). Shape perception in these stimuli arises via bottom-up integration of local components (namely similarly oriented line segments) and has been shown to involve the LO region [44]. This task was adapted from our previous TMS studies [21,33].

Materials and methods

Participants

Thirteen participants (from the fifteen participants who took part in Experiment 1, 7 males, mean age = 24.5, SD = 2.11) participated in Experiment 2.

fMRI localization and TMS

The fMRI localization procedure and the TMS parameters were the same as used in Experiment 1. The mean MNI coordinates in Experiment 2 were: *rOFA*: 39 (SD 4.5), –80 (SD 9.1), –10 (SD 2.9); *rLO*: 46 (SD 3.4), –75 (SD 4.1), –3 (SD 5.7).

Procedure

Stimuli. The stimuli consisted of Gabor patch (GP) patterns (gray scale values ranging from 13 to 165) appearing on a gray background (gray value 89) (see References 21,33). Each Gabor element was defined as the product of a sine wave luminance grating (frequency of 3.75 cycles/deg) and a two-dimensional Gaussian envelope

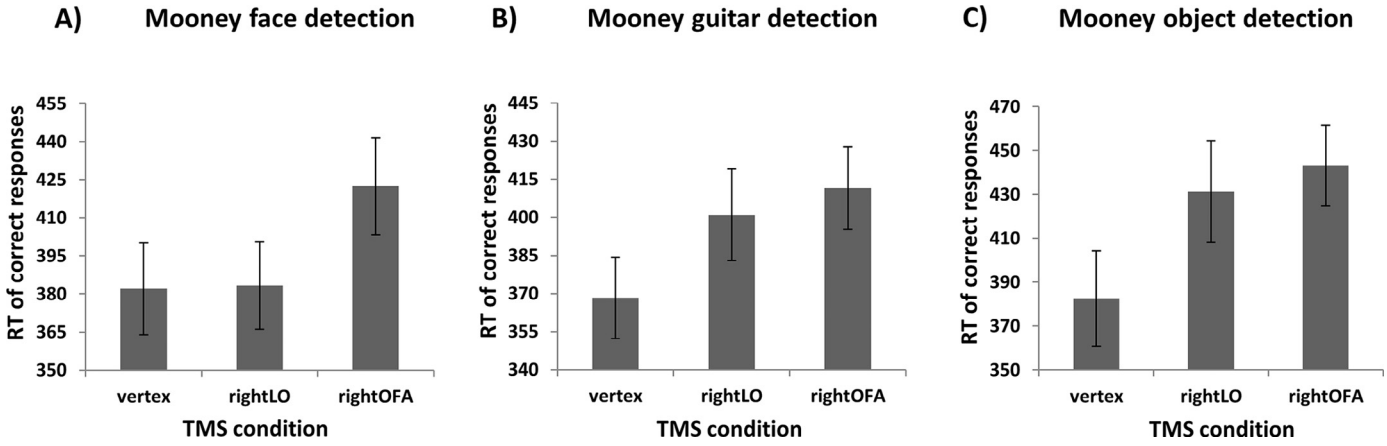

Figure 3. The mean (n = 15) reaction times of correct responses for each TMS condition in Experiment 1 for A) Mooney faces; B) Mooney guitars; C) Mooney objects. Error bars represent ±1 SEM.

(standard deviation of .19" in both dimensions). The diameter of each pattern was of 16" of visual angle and the GP diameter was .8". The number of GPs in the patterns ranged from 120 to 210 and were distributed on an invisible 20 × 20 grid. The minimum center-to-center distance between the Gabor elements was .8". A first set of 40 stimuli was created in which GPs were distributed and oriented to delineate a closed contour embedded in a random GP background (similar to Reference 45). The contour was created from a variable number of GPs that always corresponded to the 40% of the total number of GPs present on-screen (the remaining 60% of GPs were random background). A second set of 40 stimuli was generated consisting of randomly distributed and oriented GPs; for each stimulus of the first set, a corresponding random pattern was created for the second set, so that GP patterns in the two sets were carefully matched in terms of the total number of GPs they contained.

Task. Fig. 4C shows the time line of an experimental trial. Each trial started with a black fixation cross appearing in the middle of the screen for 500 ms, followed by the stimulus for 75 ms. Participants were required to indicate, with a button press, whether there was a shape present in the display. TMS site and parameters were the same with Experiment 1. Each participant carried out three blocks, one for each TMS site (rOFA, rLO and vertex). Each block contained 80 stimuli (40 with a visible shape and 40 with no shape, randomly presented). Prior to the experiment, participants underwent a brief practice (with no TMS) consisting of 20 trials (10 with a visible shape and 10 without). Both accuracy and response speed were emphasized.

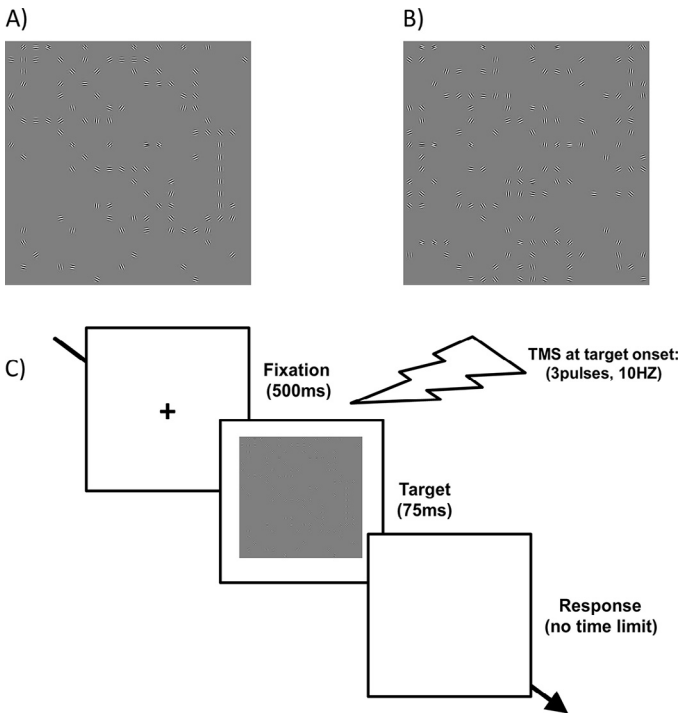

Figure 4. Experiment 2: Shape detection based on bottom-up featural processing. A) Example of a "shape present" trial; B) example of a "shape absent" trial; C) time line of an experimental trial. As in Experiment 1, participants were asked to indicate on each trial whether or not a shape was presented. TMS was applied as in Experiment 1.

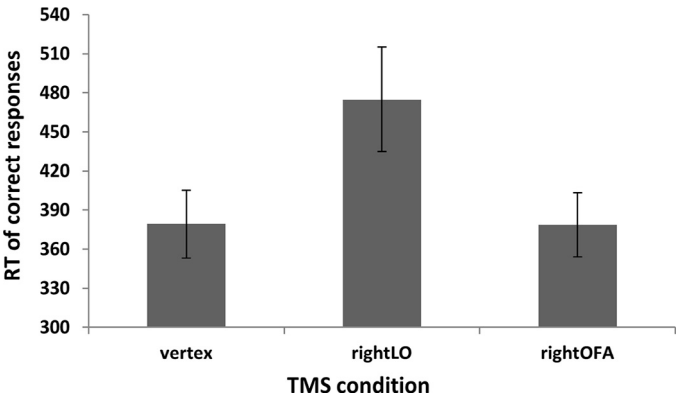

Figure 5. The mean (n = 13) reaction time of correct responses for each TMS condition in Experiment 2. Error bars represent ±1 SEM. Relative to vertex, TMS significantly impaired shape detection when applied over rLO but not over rOFA.

Results

Statistical analyses were performed on reaction times of correct responses as in Experiment 1. Mean accuracy was 87% (SD = 2.9).

Fig. 5 shows the mean reaction times of correct responses for each TMS condition. A repeated-measures ANOVA with TMS site (rLO, rOFA, vertex) as within-subjects variable showed a significant main effect of TMS, $F(2,24) = 10.71$, $p < .001$, $\eta_p^2 = .47$. Post-hoc t-tests (Bonferroni–Holm correction applied) showed that TMS over rLO significantly impaired participants' ability to detect shapes compared to vertex stimulation (control condition), $t(12) = 3.41$, $p = .01$, and to rOFA stimulation, $t(12) = 3.39$, $p = .015$. TMS over rOFA did not affect performance compared to vertex, $t(12) = .05$, $p = .96$.

Discussion

This study aimed to investigate the role of rOFA in detection of faces and objects based on holistic processing, as required by Mooney stimuli (in which recognition of the "whole" precedes detection of the single elements; see Reference 22). In Experiment 1 we applied fMRI-guided TMS over the rOFA, rLO and vertex while participants were asked to detect Mooney stimuli, which are two-tone images missing distinguishable local features and can be recognized solely with the aid of top-down guidance from previously stored representations (e.g. References 15,22,25,26,46,47). The key finding of our study is that TMS applied over rOFA impaired the detection of Mooney stimuli without category-specificity. Specifically, rOFA was found to play a role in detecting Mooney faces and guitars (which are both a homogeneous stimulus class in terms of a prototypical shapes) as well as objects of different types. Experiment 2 showed that the role of rOFA in stimulus detection may be restricted to the kind of holistic processing required by Mooney stimuli. Interfering with rLO but not with rOFA activity impaired participants' ability to detect meaningless shapes defined by a closed contour of similarly oriented Gabor elements (replicating Bona et al.'s [21] findings), whose detection is mediated by bottom-up processing of the collinearity of the single elements. The lack of rOFA effect in Experiment 2 also demonstrates that the spatial specificity of TMS was sufficient to selectively target rOFA, also in line with previous studies employing fMRI-guided TMS [12,21,35]. The statistical analysis of Experiment 1 indicates that the role of rLO in holistic detection of Mooney stimuli is not tied to any stimulus category. However, although statistical analysis did not reveal an object-selective response in rLO, a visual inspection of Fig. 3 indicates that the rLO effect was driven by an impairment of object and guitar stimuli.

The key challenge in perceiving Mooney images is that they do not contain cues to differentiate object contours from illumination effects such as shadows, unless the structure of the object has been already encountered. Accordingly, 2-tone images of unfamiliar objects cannot be perceived [23]. Object templates are crucial in Mooney stimuli detection because their recognition precedes figure-ground segregation (e.g. References 48,49). While the actual template is likely to be stored at higher-level regions, rOFA and rLO might provide input to those higher levels, and may also receive top-down guidance by the activated memory representation. The presence of certain fundamental visual features (e.g. symmetry, T-junctions for faces) that are indicative of meaningful stimulus structure can generate testable hypotheses of object identity based on existing templates (e.g. References 50,51). The key point is that many of such features are not tied to a specific category but rather could be indicators of objects of various stimulus types, such as a face, a guitar or an apple.

Our results are consistent with previous work implicating rOFA in holistic processing of faces [52–54]. For example, Jonas and colleagues [52] showed that electrical stimulation of rOFA impaired the perception of the face as a whole. Schiltz and Rossion [53] found that both FFA and OFA process face stimuli in a holistic manner, although the holistic response of OFA was weaker and less consistent across studies (cf. Reference 55). At first sight, our results appear to be inconsistent with a previous fMRI study reporting no significant BOLD response to Mooney faces in rOFA, suggesting that the detection of these stimuli might rely exclusively on higher-order visual areas such as FFA [15]. However, that conclusion relied on a contrast between upright and inverted Mooney faces (which are usually not detected as faces); this contrast would not reveal any activation that is not face selective. In other words, the role of rOFA in encoding Mooney stimuli in a non-face-selective manner would not be revealed by such analysis. Thus, our finding of rOFA's involvement in the processing of a wide range of Mooney stimuli is not in contradiction with that study.

Our results are also consistent with previous evidence pointing to a role of rOFA in processing of non-face stimuli (e.g. References 17–20; see also 56). In particular, our data fit with previous evidence suggesting that rOFA is causally involved in detection of symmetry both in faces [21,57] and in dot configurations [21,58], with symmetry discrimination being essentially holistic (e.g. References 59–61). Finally, Pitcher et al. [62] reported that TMS applied over rOFA at an early latency (40/50 ms after stimulus onset) impaired both face and body detection, whereas TMS at a later time window induced face-specific effects. The authors interpreted the earlier effect of TMS over rOFA as possibly reflecting preparatory activity in rOFA rather than target-related processing per se. In our study we did not use a chronometric approach so we cannot determine whether rOFA involvement in face and object detection reflected preparatory activity or occurred at a later stage of stimulus processing: future studies using chronometric paradigms (like References 12,35) and Mooney stimuli are needed to clarify this issue.

In conclusion, our results shed new light into the function of rOFA by showing that this region is causally involved in top-down holistic detection of Mooney stimuli and that this involvement extends beyond faces.

Acknowledgements

This work was supported by the European Research Council (grant number 336152); Emil Aaltonen Foundation and the Academy of Finland to JS and by a Fund for Investments on Basic Research (FIRB), Italian Ministry of Education, University and Research (RBFR12F0BD) to ZC. The authors wish to thank Miguel Castelo-Branco and Joao Castelhano for providing the original set of Mooney guitars from Castelhano et al. [42], Fatma Imamoglu for providing the original set of Mooney objects from Imamoglu et al. [43], and Fariba Sharifian, Simo Vanni and Hanna Heikkinen for their help in fMRI data analysis.

References

[1] Gauthier I, Tarr MJ, Moylan J, Skudlarski P, Gore JC, Anderson AW. The fusiform "face area" is part of a network that processes faces at the individual level. J Cogn Neurosci 2000;12:495–504.
[2] Haxby JV, Hoffman EA, Gobbini MI. The distributed human neural system for face perception. Trends Cogn Sci 2000;4:223–33.
[3] Ishai A, Ungerleider LG, Martin A, Haxby JV. The representation of objects in the human occipital and temporal cortex. J Cogn Neurosci 2000;2:35–51.
[4] Rossion B, Caldara R, Seghier M, Schuller AM, Lazeyras F, Mayer E. A network of occipito-temporal face-sensitive areas besides the right middle fusiform gyrus is necessary for normal face processing. Brain 2003;126:2381–95.
[5] Kadosh KC, Walsh V, Kadosh RC. Investigating face-property specific processing in the right OFA. Soc Cogn Affect Neurosci 2011;6:58–65.
[6] Haxby JV, Ungerleider LG, Clark VP, Schouten JL, Hoffman EA, Martin A. The effect of face inversion on activity in human neural systems for face and object perception. Neuron 1999;22:189–99.
[7] Rossion B, Dricot L, Devolder A, Bodart JM, Crommelinck M, De Gelder B, et al. Hemispheric asymmetries for whole-based and part-based face processing in the human fusiform gyrus. J Cogn Neurosci 2000;12:793–802.
[8] Pitcher D, Walsh V, Duchaine B. The role of the occipital face area in the cortical face perception network. Exp Brain Res 2011a;209:481–93.
[9] Rotshtein P, Henson RN, Treves A, Driver J, Dolan RJ. Morphing Marilyn into Maggie dissociates physical and identity face representations in the brain. Nat Neurosci 2005;8:107–13.
[10] Liu J, Harris A, Kanwisher N. Perception of face parts and face configurations: an FMRI study. J Cogn Neurosci 2010;22:203–11.
[11] Zhang J, Li X, Song Y, Liu J. The fusiform face area is engaged in holistic, not parts-based, representation of faces. PLoS ONE 2012;7:e40390.
[12] Pitcher D, Walsh V, Yovel G, Duchaine B. TMS evidence for the involvement of the right occipital face area in early face processing. Curr Biol 2007;17:1568–73.
[13] Dricot L, Sorger B, Schiltz C, Goebel R, Rossion B. The roles of "face" and "non-face" areas during individual face perception, evidence by fMRI adaptation in a brain-damaged prosopagnosic patient. Neuroimage 2008;40:318–32.
[14] Rossion B. Constraining the cortical face network by neuroimaging studies of acquired prosopagnosia. Neuroimage 2008;40:423–6.
[15] Rossion B, Dricot L, Goebel R, Busigny T. Holistic face categorization in higher order visual areas of the normal and prosopagnosic brain: toward a non-hierarchical view of face perception. Front Hum Neurosci 2011;4:225.
[16] Solomon-Harris LM, Mullin CR, Steeves JK. TMS to the "occipital face area" affects recognition but not categorization of faces. Brain Cogn 2013;83:245–51.
[17] Gilaie-Dotan S, Nir Y, Malach R. Regionally-specific adaptation dynamics in human object areas. Neuroimage 2008;39:1926–37.
[18] Haist F, Lee K, Stiles J. Individuating faces and common objects produces equal responses in putative face-processing areas in the ventral occipitotemporal cortex. Front Hum Neurosci 2010;4:181.
[19] Silvanto J, Schwarzkopf DS, Gilaie-Dotan S, Rees G. Differing causal roles for lateral occipital cortex and occipital face area in invariant shape recognition. Eur J Neurosci 2010;32:165–71.
[20] Slotnick SD, White RC. The fusiform face area responds equivalently to faces and abstract shapes in the left and central visual fields. Neuroimage 2013;3:408–17.
[21] Bona S, Cattaneo Z, Silvanto J. The causal role of the occipital face area (OFA) and lateral occipital (LO) cortex in symmetry perception. J Neurosci 2015;35:731–8.
[22] Latinus M, Taylor MJ. Holistic processing of faces: learning effects with Mooney faces. J Cogn Neurosci 2005;17:1316–27.
[23] Moore C, Cavanaugh P. Recovery of 3D volume from 2-tone images of novel objects. Cognition 1998;67:45–71.
[24] Mooney CM. Closure with negative after-images under flickering light. Can J Psychol 1956;10:191–9.
[25] Latinus M, Taylor MJ. Face processing stages: impact of difficulty and the separation of effects. Brain Res 2006;1123:179–87.
[26] McKeeff TJ, Tong F. The timing of perceptual decisions for ambiguous face stimuli in the human ventral visual cortex. Cereb Cortex 2007;17:669–78.
[27] Eimer M, Gosling A, Nicholas S, Kiss M. The N170 component and its links to configural face processing: a rapid neural adaptation study. Brain Res 2011;1376:76–87.
[28] Walsh V, Pascual-Leone A. Transcranial magnetic stimulation: a neurochronometrics of mind. Cambridge: MIT Press; 2003.
[29] Sack AT, Cohen Kadosh R, Schuhmann T, Moerel M, Walsh V, Goebel R. Optimizing functional accuracy of TMS in cognitive studies: a comparison of methods. J Cogn Neurosci 2009;21:207–21.
[30] Sandrini M, Umiltà C, Rusconi E. The use of transcranial magnetic stimulation in cognitive neuroscience: a new synthesis of methodological issues. Neurosci Biobehav Rev 2011;35:516–36.
[31] Miniussi C, Harris JA, Ruzzoli M. Modelling non-invasive brain stimulation in cognitive neuroscience. Neurosci Biobehav Rev 2013;37:1702–12.

[32] Oldfield RC. The assessment and analysis of handedness: the Edinburgh inventory. Neuropsychologia 1971;9:97–113.
[33] Bona S, Herbert A, Toneatto C, Silvanto J, Cattaneo Z. The causal role of the lateral occipital complex in visual mirror symmetry detection and grouping: an fMRI-guided TMS study. Cortex 2014;51:46–55.
[34] Friston KJ, Ashburner JT, Kiebel SJ, Nichols TE, Penny WD. Statistical parametric mapping: the analysis of functional brain images. Academic Press Elsevier; 2007.
[35] Pitcher D, Charles L, Devlin JT, Walsh V, Duchaine B. Triple dissociation of faces, bodies, and objects in extrastriate cortex. Curr Biol 2009;19:319–24.
[36] Pitcher D, Duchaine B, Walsh V, Yovel G, Kanwisher N. The role of lateral occipital face and object areas in the face inversion effect. Neuropsychologia 2011b;49:3448–53.
[37] Teitti S, Määttä S, Säisänen L, Könönen M, Vanninen R, Hannula H, et al. Non-primary motor areas in the human frontal lobe are connected directly to hand muscles. Neuroimage 2008;40:1243–50.
[38] Julkunen P, Säisänen L, Danner N, Niskanen E, Hukkanen T, Mervaala E, et al. Comparison of navigated and non-navigated transcranial magnetic stimulation for motor cortex mapping, motor threshold and motor evoked potentials. Neuroimage 2009;44:790–5.
[39] Saad E, Silvanto J. How visual short-term memory maintenance modulates the encoding of external input: evidence from concurrent visual adaptation and TMS. Neuroimage 2013;72:243–51.
[40] Gilaie-Dotan S, Silvanto J, Schwarzkopf DS, Rees G. Investigating representations of facial identity in human ventral visual cortex with transcranial magnetic stimulation. Front Hum Neurosci 2010;4:50.
[41] van Kemenade BM, Muggleton N, Walsh V, Saygin AP. Effects of TMS over premotor and superior temporal cortices on biological motion perception. J Cogn Neurosci 2012;24:896–904.
[42] Castelhano J, Rebola J, Leitão B, Rodriguez E, Castelo-Branco M. To perceive or not perceive: the role of gamma-band activity in signaling object percepts. PLoS ONE 2013;8:e66363.
[43] Imamoglu F, Kahnt T, Koch C, Haynes JD. Changes in functional connectivity support conscious object recognition. Neuroimage 2012;63:1909–17.
[44] Kourtzi Z, Tolias AS, Altmann CF, Augath M, Logothetis NK. Integration of local features into global shapes: monkey and human FMRI studies. Neuron 2003;37:333–46.
[45] Kourtzi Z, Betts LR, Sarkheil P, Welchman AE. Distributed neural plasticity for shape learning in the human visual cortex. PLoS Biol 2005;3:e204.
[46] Moscovitch M, Winocur G, Behrmann M. What is special about face recognition? Nineteen experiments on a person with visual agnosia and dyslexia but normal face recognition. J Cogn Neurosci 1997;9:555–604.
[47] McKone E. Isolating the special component of face recognition: peripheral identification and a Mooney face. J Exp Psychol Learn Mem Cogn 2004;30:181–97.
[48] Cavanagh P. Short-range vs long-range motion: not a valid distinction. Spat Vis 1991;5:303–9.
[49] Peterson MA, Gibson BS. Object recognition contributions to figure-ground organization: operations on outlines and subjective contours. Percept Psychophys 1994;56:551–64.
[50] Gibson JJ. The ecological approach to visual perception. Boston: Houghton Mifflin; 1979.
[51] Biederman I. Recognition-by-components: a theory of human image understanding. Psychol Rev 1987;4:115–47.
[52] Jonas J, Descoins M, Koessler L, Colnat-Coulbois S, Sauvée M, Guye M, et al. Focal electrical intracerebral stimulation of a face-sensitive area causes transient prosopagnosia. Neuroscience 2012;222:281–8.
[53] Schiltz C, Rossion B. Faces are represented holistically in the human occipito-temporal cortex. Neuroimage 2006;32(3):1385–94.
[54] Kovács G, Cziraki C, Vidnyánszky Z, Schweinberger SR, Greenlee MW. Position-specific and position- invariant face aftereffects reflect the adaptation of different cortical areas. Neuroimage 2008;43:156–64.
[55] Schiltz C, Dricot L, Goebel R, Rossion B. Holistic perception of individual faces in the right middle fusiform gyrus as evidenced by the composite face illusion. J Vis 2010;10:25, 1-16.
[56] Renzi C. Ferrari C, Schiavi S, Pisoni A, Papagno C, Vecchi T, et al. The role of the occipital face area in holistic processing involved in face detection and discrimination: a tDCS study. Neuropsychology 2015;29:409–16.
[57] Chen CC, Kao KL, Tyler CW. Face configuration processing in the human brain: the role of symmetry. Cereb Cortex 2007;17:1423–32.
[58] Sasaki Y, Vanduffel W, Knutsen T, Tyler C, Tootell R. Symmetry activates extrastriate visual cortex in human and nonhuman primates. Proc Natl Acad Sci USA 2005;102:3159–63.
[59] Wagemans J. Characteristics and models of human symmetry detection. Trends Cogn Sci 1997;1(9):346–52.
[60] Rhodes G, Peters M, Ewing LA. Specialised higher-level mechanisms for facial-symmetry perception: evidence from orientation-tuning functions. Perception 2007;36:1804–12.
[61] Treder MS. Behind the looking-glass: a review on human symmetry perception. Symmetry 2010;2:1510–43.
[62] Pitcher D, Goldhaber T, Duchaine B, Walsh V, Kanwisher N. Two critical and functionally distinct stages of face and body perception. J Neurosci 2012;32:15877–85.